Characteristics and implications of CO_2/CH_4 mixtures adsorbing on shale kerogen: molecular simulation [#]

Zhongqi Mu[1,2], Zhengfu Ning[1,2*], Bei Liu[3]

1 State Key Laboratory of Petroleum Resources and Prospecting, China University of Petroleum, Beijing 102249, China

2 Key Laboratory of Petroleum Engineering of the Ministry of Education, China University of Petroleum, Beijing 102249, China

3 State Key Laboratory of Heavy Oil Processing, China University of Petroleum, Beijing 102249, China

ABSTRACT

Understanding the adsorption behaviors of CO_2 and CH_4 is of significance to exploit shale gas by CO_2 injection. This paper simulates the adsorption of pure CO_2, CH_4 and their mixtures on kerogen for different pressures and compositions. The stability of adsorption, the affinity between gas and kerogen, and the efficiency of injecting CO_2 to displace adsorbed CH_4 are discussed. Results show that kerogen adsorbs CO_2 more preferentially than CH_4. The presence of CO_2 causes a minimum and maximum in the adsorption isotherms of CH_4 with increasing pressure. CO_2 is adsorbed more stably than CH_4 overall but adsorbed CO_2 molecules are more heterogeneous in stability than CH_4. The increasing pressure and CO_2 mole fraction in free gas result in the decrease in adsorption selectivity of CO_2 over CH_4 under high pressure, while the trends are reversed under low pressure. Within the exploitable pressure range, the effects of injecting CO_2 for displacing adsorbed CH_4 are similar between different reservoir pressures. The adsorbed CH_4 will be displaced more intensively in the early stage of CO_2 injection than other stages. This research provides some recognitions for recovering shale gas by injecting CO_2.

Keywords: carbon dioxide, shale gas, adsorption, carbon utilization, carbon storage, molecular simulation

NOMENCLATURE

Symbols	
S_{CO_2/CH_4}	CO_2/CH_4 adsorption selectivity
x_{CO_2}	CO_2 mole fraction in adsorbed gas
x_{CH_4}	CH_4 mole fraction in adsorbed gas
y_{CO_2}	CO_2 mole fraction in free gas
y_{CH_4}	CH_4 mole fraction in free gas
E_{CO_2/CH_4}	Efficiency of CO_2 displacing adsorbed CH_4

1. INTRODUCTION

Shale gas reservoirs are mainly developed by depletion, which brings the problems of fast decline and low productivity.[1] CO_2 injection is an innovative method still in the theoretical research stage. Not only can applying this method replenish the energy of reservoirs, but it can also displace the adsorbed gas employing the difference in adsorption between CO_2 and CH_4.[1] The advances and popularization of CO_2 injection technology for producing shale gas are of great significance to the storage and utilization of carbon.

At present, there are many experimental studies on the adsorption of CO_2 and CH_4 on shale, which mainly focus on the adsorption of pure gas.[2-4] Relevant results demonstrate that shale has a stronger adsorption affinity for CO_2 than CH_4. Qi et al.[5] measures the adsorption quantities of CO_2/CH_4 mixtures on shale, which also prove the preferential adsorption of CO_2 but finds the adsorption affinity for CO_2 predicted by pure gas much higher than that in the competitive adsorption. There are few experimental studies on the adsorption of CO_2/CH_4 mixtures and more researches are required.

Organic matter contributes to the majority of micropores in shale and provides a large area of adsorbable surface. Therefore, organic matter pores are the main places for the storage of adsorbed gas,[6, 7] and studies on the competitive adsorption of CO_2 and CH_4 mostly focus on organic matter. Huang et al.[8, 9] studies the effects of shale kerogen type, maturity and water content on the adsorption of CO_2/CH_4 mixtures by molecular simulation, and determines the most suitable kerogen type for CO_2 storage. Further, Wang et al.[10] determines the optimal burial depth for injecting CO_2 based on the adsorption selectivity of CO_2 over CH_4 and desorption quantity of CH_4 in kerogen. Nevertheless, gas injection is long-term and the dynamic change of

adsorbed CH$_4$ displaced by CO$_2$ requires further concerns.

This paper first simulates the adsorption of pure CO$_2$, CH$_4$ and their mixtures on kerogen under the condition of middle and shallow shale gas reservoirs in Wufeng and Longmaxi formation in Sichuan Basin, China. Then, the adsorption stability and affinity of gas on kerogen are analyzed, as well as the dynamic process of injecting CO$_2$ to displace adsorbed CH$_4$. Some understandings are finally proposed for the exploitation of shale gas by injecting CO$_2$.

2. SIMULATIONS FOR GAS ADSORPTION IN KEROGEN

2.1 Models of kerogen and gas

The software of Materials studio was applied for the simulations. The type IID kerogen molecule established by Ungerer et al[11] was selected for constructing the kerogen model. Under 300 K, 16 geometric-optimized kerogen molecules were integrated into a cubic lattice with a side length of 8.69 nm and initial density of 0.1 g/cm^3. A final kerogen construction was then obtained by molecular dynamics. Firstly, 10 annealing cycles were conducted under the NVT ensemble, where the temperature increased from 300 K to 800 K and then decreased to 300 K in each cycle. A heating or cooling process was composed of 5 processes, each of which lasted 10 ps, and the total simulation time was 1 ns. Secondly, the model was relaxed at 800 K for 400 ps under the NVT ensemble. Then, under 80 MPa, the simulations were conducted under the NPT ensemble at 800 K, 600 K, 400 K, and 300 K successively with a duration of 400 ps each time. Finally, the NPT ensemble was used to simulate for 1 ns under typical reservoir conditions (363 K, 30 MPa) to obtain the final construction (Fig.1). In the above simulations, the Nosé method is used for temperature control and Berendsen method for pressure control. The final model is in a side length of 3.71 nm. The apparent density, 1.28 g/cm^3, is close to the measured values of high mature kerogen of 1.18~1.25 g/cm^3.[12] The porosity measured with helium is 8.9%, consistent with those of the organic matter of Barnett shale calculated from SEM (scanning electron microscope) images ranging from 4.5% to 22.5%.[13] Each CH$_4$ or CO$_2$ molecular is modeled as an all-atom model.
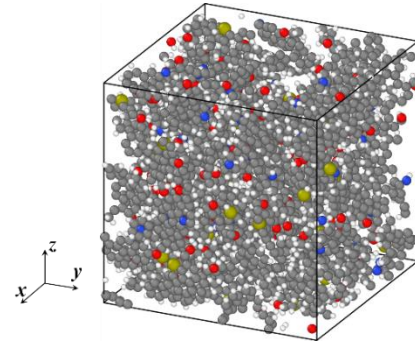

Fig. 1 Kerogen model (grey for carbon, white for hydrogen, red for oxygen, blue for nitrogen, and yellow for sulfur)

2.2 Simulation process

According to the geological conditions of the middle and shallow shale reservoirs in southern Sichuan Basin, China,[14] the simulations are determined to be conducted under the pressures of 0~30 MPa and temperature of 363 K. The Grand Canonical Monte Carlo (GCMC) method is applied to determine the average number of adsorbed CH$_4$ molecules in the kerogen. The fugacity of the gas is calculated in the Reference Fluid Thermodynamic and Transport Properties Database (REFPROP) from National Institute of Standards and Technology (NIST).

Periodic boundary conditions are applied in the x-, y- and z-directions. The time step is set to 1 fs for each simulation. The time for equilibrium and production in simulations are set as 2 ns and 10 ns respectively. The force field used is COMPASS. The summation for electrostatic interaction is accomplished through Ewald method with computing accuracy of 0.001 kcal/mol. The summation for van der Waals force is completed through Atom-based method with cutoff radius of 18.5Å.

3. THEORETICAL ANALYSIS

The adsorption selectivity indicates the preference of the adsorbent to different adsorbates. CO$_2$/CH$_4$ adsorption selectivity is defined as follows:[8, 9]

$$S_{CO_2/CH_4} = \frac{x_{CO_2}/x_{CH_4}}{y_{CO_2}/y_{CH_4}}$$

In the actual production of shale gas with CO$_2$ injection, the dynamic process of displacing adsorbed CH$_4$ with CO$_2$ continuously is also noteworthy. Here we define the average efficiency of injected CO$_2$ displacing adsorbed CH$_4$ for the process from state 1 to state 2 as the ratio of the increase in the CO$_2$ mole fraction in adsorbed gas to that in free gas:

$$(E_{CO_2/CH_4})_{1\rightarrow2} = \frac{(x_{CO_2})_2 - (x_{CO_2})_1}{(y_{CO_2})_2 - (y_{CO_2})_1}$$

Where the subscripts indicate different states.

4. RESULTS AND DISCUSSIONS

4.1 Adsorption quantity

Fig.2 shows the adsorption isotherms of CH_4 and CO_2 under different mole fractions of CO_2 in free gas. It is found that the increasing CO_2 mole fraction in free gas leads to a natural decrease in CH_4 adsorption and increase in CO_2 adsorption. The adsorption isotherms of CH_4 and CO_2 are approximately Langmuir type for the pure gas adsorption. In the adsorption of gas mixtures, the isotherms of CO_2 are still approximately Langmuir type. However, the adsorption quantity of CH_4 do not increase monotonically with pressure but first appears a minimum at 5 MPa and then appears a maximum at 25 MPa. This indicates a complex adsorption behavior of CH_4/CO_2 mixtures in kerogen.
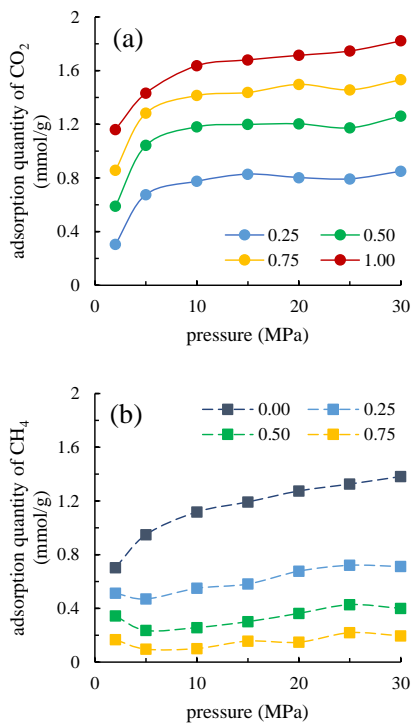
Fig. 2 Adsorption isotherms of (a) CH_4 and (b) CO_2 under different CO_2 mole fractions in free gas

4.2 Stability of adsorption

The energy of the adsorbed molecules reflects the stability of adsorption. Fig.3 shows the energy distribution of adsorbed gas under different CO_2 mole fractions in free gas and different pressures. It is observed that the energy distribution curves of CH_4 are basically overlapped, as well as those of CO_2. This indicates that the composition and pressure of gas mixture hardly affect the stability of each adsorbed component. The average energy of adsorbed CH_4 is significantly higher than that of CO_2, suggesting that adsorbed CH_4 is not as stable as adsorbed CO_2. This can be used to explain why CO_2 is more easily adsorbed in

kerogen than CH_4 from the perspective of energy. Moreover, the range of energy distribution of adsorbed CH_4 is narrower than that of adsorbed CO_2, which shows that the adsorbed CH_4 molecules are more uniform in energy than adsorbed CO_2 molecules. This indicates a smaller difference in adsorption stability between different CH_4 molecules, which might result from the different molecular structures. To be specific, CH_4 molecules are tetrahedral and the difference between different adsorption states is small, while CO_2 molecules are straight and being adsorbed in tiled and vertical state are obviously different.
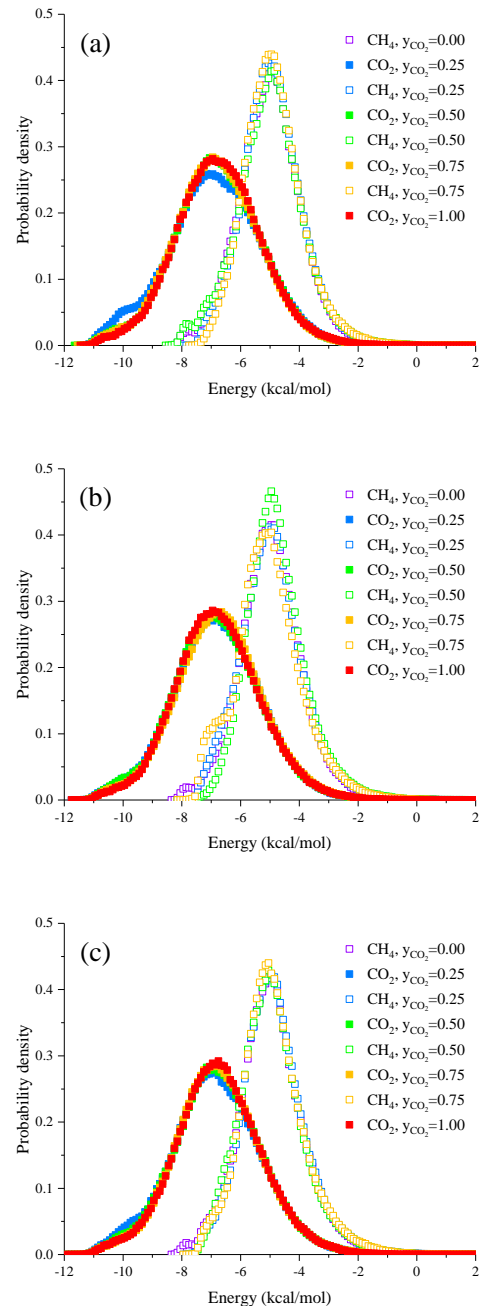
Fig. 3 Energy distribution of adsorbed gas under (a) 5 MPa, (b) 15 MPa and (c) 30MPa

4.3 Adsorption Selectivity

Fig.4 shows the adsorption selectivity changing with the pressure and CO_2 mole fraction in free gas. Under different pressures, the adsorption selectivity of CO_2 over CH_4 is generally much larger than 1, proving a much stronger adsorption affinity of kerogen to CO_2 than that to CH_4. For each CO_2 mole fraction in free gas, with the increasing pressure, the adsorption selectivity increases rapidly at first, reaches a maximum for pressure between 5 MPa and 10 MPa, and decreases slowly. Besides, the change of the adsorption selectivity with the CO_2 mole fraction in free gas is reversed with increasing pressure. A larger CO_2 mole fraction in free gas induces a larger adsorption selectivity for pressure less than 10 MPa while a smaller adsorption selectivity for pressure higher than 15 MPa. These have been reported by previous studies and are generally attributed to the surface heterogeneity of kerogen.[8, 9] Specifically, strong adsorption sites tend to be occupied by CO_2 more preferentially than weak sites. Under low pressure, many strong adsorption sites can still accommodate adsorbed gas, and the increasing pressure or CO_2 mole fraction in free gas promotes CO_2 to further occupy more strong sites, thus enhancing the overall affinity of kerogen to CO_2. Under high pressure, however, unoccupied strong adsorption sites are few and this induces CO_2 and CH_4 to compete more for weak adsorption sites, resulting in a weaker overall affinity.
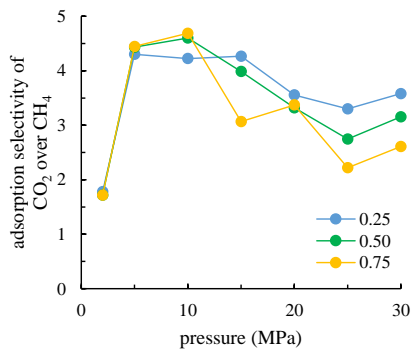

Fig. 4 Adsorption selectivity of CO_2 over CH_4 under different CO_2 mole fractions in free gas

4.4 Average efficiency of CO_2 displacing adsorbed CH_4

The process of displacing adsorbed CH_4 with CO_2 is divided into four stages according to the CO_2 mole fraction in free gas: stage I for $0 \leq y_{CO_2} < 0.25$, stage II for $0.25 \leq y_{CO_2} < 0.5$, stage III for $0.5 \leq y_{CO_2} < 0.75$, and stage IV for $0.75 \leq y_{CO_2} \leq 1$. The average displacement efficiency for each stage is demonstrated in Fig. 5. It is noted that the displacement efficiency for pressure of 2 MPa is obviously different from those for pressure higher than 5

MPa. Generally, it is difficult to exploit a shale gas reservoir till the pressure is lower than 5 MPa. Within the exploitable pressure range (>5 MPa), the difference in the average displacement efficiency between different stages is found to be little under different pressures. This implicates that for a shale gas reservoir with original pressure of 30 MPa and temperature of 363 K, there is little difference in the effect of injecting CO_2 for displacing adsorbed CH_4 between different reservoir pressures. From the stage I to stage IV, the average displacement efficiency decreases. The average displacement efficiencies for the stage I are up to 2.10~2.35, while those for the other stages are smaller than 1. These indicate that the effect of displacing adsorbed CH_4 becomes worse with the continuous CO_2 injection, and the production of adsorbed CH_4 displaced by CO_2 is mainly concentrated in the early stage of gas injection.
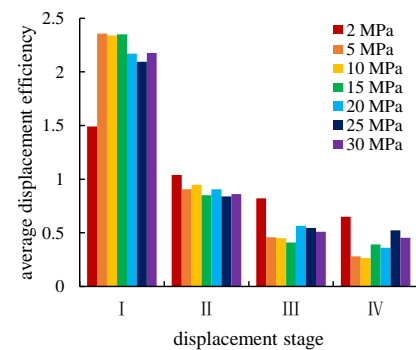

Fig. 5 Average efficiency of CO_2 displacing adsorbed CH_4

5. CONCLUSIONS

Pure CH_4, CO_2 and their mixtures are simulated to adsorb in overmature kerogen. Following results and recognitions are summarized:

(1) Increasing CO_2 mole fraction in free gas results in a decrease in CH_4 adsorption. For the adsorption of gas mixtures, the isotherms of CO_2 correspond to the Langmuir type approximately, but each of those for CH_4 exists a minimum and maximum successively with increasing pressure.

(2) The stability of adsorbed gas is independent to the composition of free gas and pressure. CO_2 is adsorbed more stably than CH_4 overall but CO_2 molecules are more heterogeneous in adsorption stability than CH_4.

(3) The adsorption selectivity of CO_2 over CH_4 is generally much larger than 1, indicating that kerogen adsorbs CO_2 more preferentially than CH_4. The adsorption selectivity increases rapidly with the increasing pressure for pressure lower than 5~10 MPa and decreases slowly for higher pressure. For pressure lower than 10~15 MPa, the adsorption selectivity

increases with the increasing CO_2 mole fraction in free gas, but the trend is reversed for higher pressure.

(4) Within the exploitable pressure range, the effects of injecting CO_2 for displacing adsorbed CH_4 are similar between different reservoir pressures. The average efficiency of CO_2 displacing adsorbed CH_4 for the early gas-injection stage are far higher than those for the other stages, which implies that the adsorbed CH_4 will be produced intensively in the early stage of gas injection.

REFERENCE

[1] Du F, Nojabaei B. A Review of Gas Injection in Shale Reservoirs: Enhanced Oil/Gas Recovery Approaches and Greenhouse Gas Control. ENERGIES. 2019;12:2355.

[2] Zhou J, Liu M, Xian X, Jiang Y, Liu Q, Wang X. Measurements and modelling of CH4 and CO2 adsorption behaviors on shales: Implication for CO2 enhanced shale gas recovery. FUEL. 2019;251:293-306.

[3] Qi R, Ning Z, Wang Q, Huang L, Wu X, Cheng Z, et al. Measurements and modeling of high-pressure adsorption of CH4 and CO2 on shales. FUEL. 2019;242:728-743.

[4] Hu K, Herdegen V, Mischo H. Carbon dioxide adsorption to 40 MPa on extracted shale from Sichuan Basin, southwestern China. FUEL. 2022;318:123666.

[5] Qi R, Ning Z, Wang Q, Zeng Y, Huang L, Zhang S, et al. Sorption of Methane, Carbon Dioxide, and Their Mixtures on Shales from Sichuan Basin, China. ENERG FUEL. 2018;32:2926-2940.

[6] Ju Y, He J, Chang E, Zheng L. Quantification of CH4 adsorption capacity in kerogen-rich reservoir shales: An experimental investigation and molecular dynamic simulation. ENERGY. 2019;170:411-422.

[7] Feng G, Zhu Y, Wang GGX, Chen S, Wang Y, Ju W. Supercritical Methane Adsorption on Overmature Shale: Effect of Pore Structure and Fractal Characteristics. ENERG FUEL. 2019;33:8323-8337.

[8] Huang L, Ning Z, Wang Q, Zhang W, Cheng Z, Wu X, et al. Effect of organic type and moisture on CO2/CH4 competitive adsorption in kerogen with implications for CO2 sequestration and enhanced CH4 recovery. APPL ENERG. 2018;210:28-43.

[9] Huang L, Ning Z, Wang Q, Qi R, Zeng Y, Qin H, et al. Molecular simulation of adsorption behaviors of methane, carbon dioxide and their mixtures on kerogen: Effect of kerogen maturity and moisture content. FUEL. 2018;211:159-172.

[10] Wang T, Tian S, Li G, Sheng M. Selective adsorption of supercritical carbon dioxide and methane binary mixture in shale kerogen nanopores. J NAT GAS SCI ENG. 2018;50:181-188.

[11] Ungerer P, Collell J, Yiannourakou M. Molecular Modeling of the Volumetric and Thermodynamic Properties of Kerogen: Influence of Organic Type and Maturity. ENERG FUEL. 2015;29:91-105.

[12] Okiongbo KS, Aplin AC, Larter SR. Changes in Type II Kerogen Density as a Function of Maturity: Evidence from the Kimmeridge Clay Formation. ENERG FUEL. 2005;19:2495-2499.

[13] Loucks RG, Reed RM, Ruppel SC, Jarvie DM. Morphology, Genesis, and Distribution of Nanometer-Scale Pores in Siliceous Mudstones of the Mississippian Barnett Shale. J SEDIMENT RES. 2009;79:848-861.

[14] He X, Li W, Dang L, Huang S, Wang X, Zhang C, et al. Key technological challenges and research directions of deep shale gas development. Natural Gas Industry. 2021;41:1-7.